35th Annual International Conference of the IEEE EMBS
Osaka, Japan, 3 - 7 July, 2013

A Simplified Biophysical Cell Model For Gastric Slow Wave Entrainment Simulation

Peng Du[1] and Jerry Gao[1] and Gregory O'Grady[1,2] and Leo K. Cheng[1,3]

Abstract— **Gastric electrical activity, also termed slow wave activity, is generated by a class of pacemaker cells called the interstitial cells of Cajal (ICC), which are organized with decreasing intrinsic frequencies along the stomach. In the healthy stomach, slow waves of different intrinsic frequencies converge to a single frequency with a constant phase-lag, in a process called entrainment. The main aim of this study was to develop a simplified biophysical ICC model that is capable of modeling the self-excitatory behavior and standard morphology of gastric slow waves. Entrainment of gastric slow waves was simulated in a one-dimensional (1D) model, with a linear gradient of intrinsic slow wave frequencies. In a coupled 1D model, the simulated slow waves were entrained to a single frequency; whereas in an uncoupled 1D model, the simulated slow waves occurred at different frequencies, resulting in loss of entrainment. The new cell model presents an option for future large multi-scale simulations of gastric slow waves in intact ICC network and diseased conditions where the loss of entrainment may lead to slow wave dysrhythmias and diminished gastric motility.**

I. INTRODUCTION

Gastrointestinal (GI) motility is an important component of digestive health. In particular, diminished gastric motility may contribute to a number of clinically significant diseases, such as gastroparesis (delayed emptying), slow transit, and gastro-eosophageal reflux disease (GERD) [1]. One major regulatory component of gastric motility is an underlying rhythmic electrical activity called slow waves, which are generated by the Interstitial cell of Cajal (ICC) [2]. ICC are distributed throughout the stomach and other parts of the GI tract, acting as electrical pacemakers that are capable of synchronization of slow waves with different intrinsic frequencies to a single frequency, i.e., entrainment, under normal conditions [3]. In the healthy human stomach, the entrained slow wave frequency is around 3 cycles-per-minute (cpm) [4]. On the other hand, under pathological conditions, e.g., gastroparesis, ICC counts are known to reduce and result in loss of entrainment, contributing to the development of gastric slow wave dysrhythmias [5,6].

*This work was supported in part by the New Zealand Health Research Council (HRC), and the US National Institutes of Health (R01 DK64775). Peng Du is supported by a Rutherford Foundation New Zealand Postdoctoral Fellowship and a Marsden Fast-Start Grant. Jerry Gao is supported by a University of Auckland Health Research Doctoral Scholarship, a Freemasons Postgraduate Scholarship, and a R.H.T. Bates Postgraduate Scholarship.

[1]P. Du, J. Gao, G. O'Grady, and L.K. Cheng are with Auckland Bioengineering Institute, the University of Auckland, NZ; peng.du@auckland.ac.nz

[2]G. O'Grady is also with Department of Surgery, the University of Auckland, NZ

[3]L.K. Cheng is also with Department of Surgery, Vanderbilt University, Nashville, TN, USA

Improved understanding of the ICC pacemaking mechanisms has led to recent development of many biophysical slow wave cell models [7-9]. However, most of these biophysical cell models contain a large number of ordinary differential equations (ODEs) and parameters that make their applications in large-scale multi-scale slow wave propagation simulations computationally intractable. Investigators have also modeled the electrical activity of gastric smooth muscle cell [10].

The main aim of this study was to develop a more computationally efficient model of ICC slow wave activity. Three main aspects were considered: (i) the biophysical basis of the ion conductances included in the model; (ii) the ability of the cell model to generate intrinsic rhythmic gastric slow wave activity; and (iii) the applicability of cell model to simulate entrainment in a continuum model.

II. MODEL DEVELOPMENT

A. Cell Model

Of the many biophysical cell models of GI slow wave activity [7-9], the model developed by Imtiaz *et al.* was used as the template to update and parameterize the new model [11]. The original cell model included a generic I_{ion} component that was updated using a Ca^{2+}-dependent K^+ conductance (I_{BK}) and Na^+ conductance (I_{Na}) proposed by Corrias *et al.* [7], which retained as much biophysical basis for these ion conductances as possible. A stimulus current (I_s) was also added to the equation to demonstrate the response of the cell to an extrinsic current.

$$C_m \frac{dV_m}{dt} = I_{Na} + I_{Ca} + I_{BK} - I_s \tag{1}$$

where I_{Na} was described using a standard Hodgkin-Huxley gating approach [7].

$$I_{Na} = G_{Na} f_{Na} d_{Na} (V_m - E_{Na}) \tag{2}$$

$$\frac{d_{Na}}{dt} = \frac{d_{inf} - d_{Na}}{\tau_{d_{Na}}} \tag{3}$$

$$d_{inf} = \frac{1}{1 + \exp^{\frac{V_m+7}{-5}}} \tag{4}$$

$$\frac{f_{Na}}{dt} = \frac{f_{inf} - f_{Na}}{\tau_{f_{Na}}} \tag{5}$$

$$f_{inf} = \frac{1}{1 + \exp^{\frac{V_m+37.4}{4}}} \tag{6}$$

I_{BK} was regulated by a Ca^{2+}-dependent gating variable (d_{BK}) [7].

$$I_{BK} = G_{BK} d_{BK} (V_m - E_K) \tag{7}$$

$$d_{BK} = \frac{1}{1 + e^{\frac{V_m}{-17} - 2ln\frac{Ca_c}{0.001}}} \tag{8}$$

I_{Ca} was modeled as Hill-type activation conductance (G_{Ca}) [11].

$$I_{Ca} = G_{Ca}(V_m - E_{Ca}) \tag{9}$$

$$G_{Ca} = G_{MCa} \frac{Ca_c^q}{k_C a^q + Ca_c^q} \tag{10}$$

The intracellular calcium dynamic was modeled as a two-pool system (cytosol store (Ca_c) and mitochondrial store (Ca_s)) using the following set of equations [11],

$$V_{in} = V_0 + V_1 IP_3 \tag{11}$$

$$V_2 = V_{M2} \frac{Ca_c^n}{k_2^n + Ca_c^n} \tag{12}$$

$$V_3 = V_{M3} \frac{Ca_c^w}{k_a^w + Ca_c^w} \frac{Ca_s^m}{k_r^m + Ca_s^m} \frac{IP_3^o}{k_p^o + IP_3^o} \tag{13}$$

$$\frac{IP_3}{dt} = \beta - \eta IP_3 - V_{M4} \frac{IP_3^u}{k_4^u + IP_3^u} + P_{MV} \frac{V_m^r}{k_v^r + V_m^r} \tag{14}$$

$$\frac{Ca_s}{dt} = V_2 - V_3 - k_f Ca_s \tag{15}$$

$$\frac{Ca_s}{dt} = V_{in} - V_2 + V_3 + k_f Ca_s - KCa_c \tag{16}$$

The parameter descriptions and values used to simulate gastric slow wave activity are presented in the Appendix (Table II).

B. One-Dimensional Entrainment Model

A one-dimensional (1D) model geometric model with a linear basis function was created to model entrainment of gastric slow waves. The 1D model was 10 mm in length, and contained 101 cells, with each cell presenting a solution point, which gives a spatial resolution of 0.1 mm (Fig. 1(a)). An intrinsic frequency gradient was assigned linearly to the 1D model, from 3 cpm at the left-hand-side of the model (proximal) to 2.5 cpm at the right-hand-side of the model (distal). The proximal end corresponded to the corpus (mid-stomach) and the distal end corresponded to the region towards the antrum. The parameter β in Eqn 8 was adjusted to match this frequency range (Fig. 1(b)).

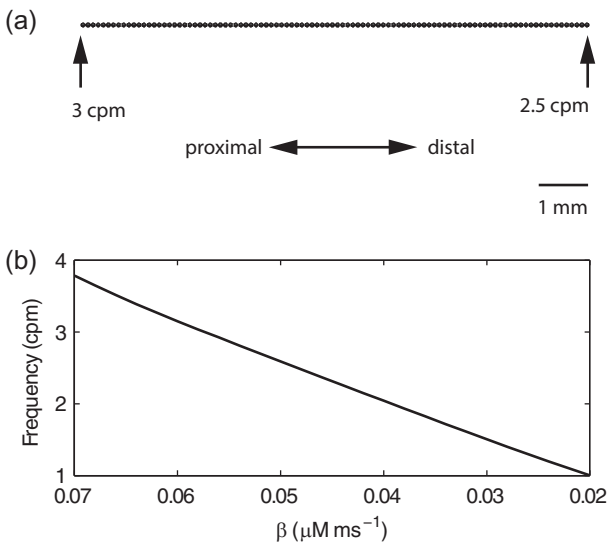

Fig. 1. One-dimensional entrainment model setup. (a) Locations of solution points, a linear gradient of instrinsic frequencies (2.5-3 *cpm*) were assigned to the model. (b) The effect of varying parameter β on simulated slow wave frequency.

The bidomain equations (illustrated in Fig. 2) were solved to simulate slow wave propagations [12], as have been previously applied [13,14].

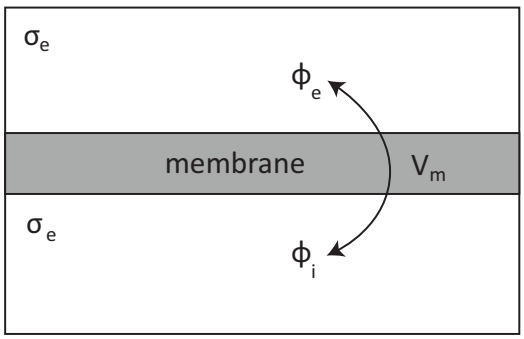

Fig. 2. An illustration of the bidomain model. The transmembrane potential (V_m) across a cell membrane is the potential difference between an extracellular potential (ϕ_e) and an intracellular potential (ϕ_i). Each domain also contains a conductivity tensor, σ_e in the extracellular domain and σ_i in the intracellular domain

The bidomain equations are,

$$\nabla \cdot (\sigma_i \nabla V_m) = -\nabla \cdot ((\sigma_i + \sigma_e) \nabla \phi_e) \tag{17}$$

$$A_m (C_m \frac{\partial V_m}{\partial t} + I_{ion}) - \nabla(\sigma_i \phi_e) = \nabla \cdot (\sigma_i \nabla V_m) \tag{18}$$

where the σ terms denote tissue conductivity tensors, with subscript i denoting the intracellular domain and subscript e denoting the extracellular domain; A_m denotes the cell-surface-to-volume ratio (200 mm^{-1}) and I_{ion} denotes the current flow through the cell membrane, as described in Eqn 1. The no-flux boundary condition was used.

Two cases were simulated: (i) coupled tissue, where the conductivity values were set to 15 $mS\,mm^{-1}$; (ii) uncoupled tissue, where the conductivity values were reduced to

4 $mS\,mm^{-1}$. A period of 360 s of slow wave propagation was simulated for each case on a single processor of an IBM p595 HPC. The first 120 s was discarded to allow the model to reach a steady-state. A previous 1D model developed by Du *et al.* was also applied in the same setup to compare computational efficiency [13].

III. RESULTS AND DISCUSSION

A. Cell Model

The simulated slow wave membrane potential exhibited the following features: frequency: 3 cpm, resting membrane potential: -70 mV, and peak potential: -40 mV (Fig. 3(a)). When a 10 μA stimulus current was applied, the phase of the simulated slow wave was advanced (Fig. 3(b)). The new cell model also exhibited a degree of inverse correlation between the intrinsic frequency and amplitude, with lower frequencies leading to higher amplitudes (Fig. 3(c)).

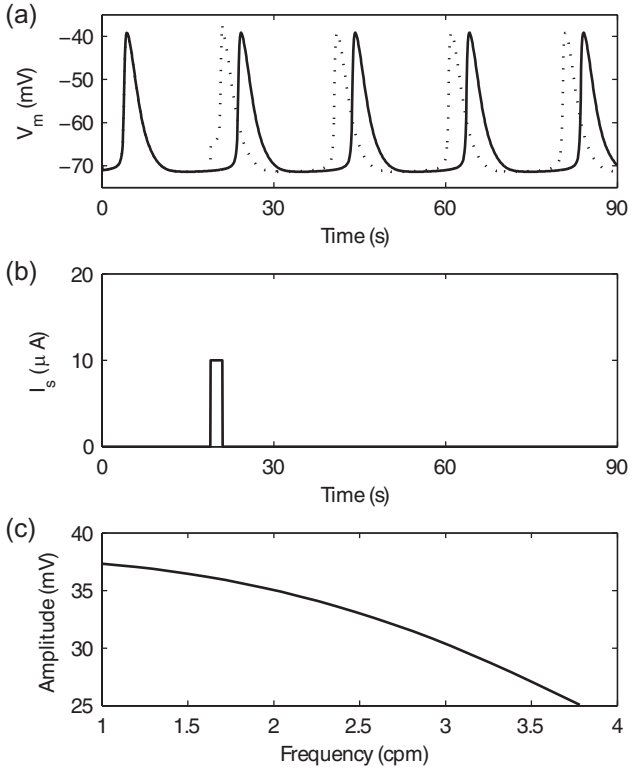

Fig. 3. Cell model simulations. (a) Simulated gastric slow wave at an intrinsic frequency of 3 cpm (solid line). (b) A 10 μA stimulus was injected at 19 s, the phase of the subsequent simulated slow wave was advanced (dashed line in (a)). (c) Frequency-amplitude relationship of the slow wave simulated by the cell model.

The new cell model contained six ODEs and 35 parameters, which was significantly fewer than the three aforementioned biophysical cell models, as shown in Table I. All six ODEs were tested and solved for during computation. A period of 60 s of slow wave activity was simulated and each ODE was solved using a forward Euler method with a fixed time step of 0.01 ms on an Intel i5 M460 core. Higher-order solvers such as the Runge-Kutta method could also be applied to solve the system of ODEs.

TABLE I
SLOW WAVE CELL MODELS.

Cell Model	ODEs	Parameters	Solution Time (s)
Faville *et al.* [6]	78	640	83.9
Corrias *et al.* [5]	22	116	21.3
Youm *et al.* [7]	14	53	16.2
new model	6	35	10.2

Compared to the existing biophysical cell models listed in Table I, the new cell model was computationally more efficient; however, even though the new cell model demonstrated a comparable morphology to experimental data [2], the main trade-off was that the detailed morphology, e.g., the plateau phase, was not as accurate as the more complicated biophysical cell models [7-9]; this difference could be attributed to the exclusion of the detailed ion conductances, such as the L-type Ca^{2+} channel [7], from the cell model.

B. Entrainment Model

Slow wave entrainment was simulated as a coupled system of ICC in a 1D model (Fig. 4).

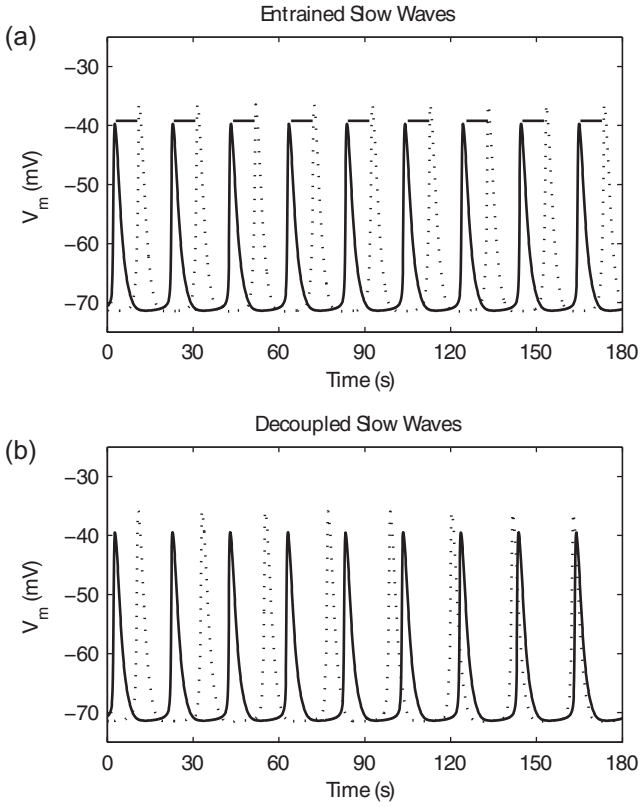

Fig. 4. Slow wave propagation simulations. The simulated slow waves at the ends of the 1D model are shown (proximal: solid-line; distal: dashed-line). (a) Entrainment was simulated in the coupled system. The entrainment frequency was 3 cpm. The constant phase-locking is indicated by the solid horizontal lines. (b) Loss-of-entrainment was achieved by reducing the conductivities. The simulated slow waves occurred at different frequencies (3 cpm and 2.8 cpm).

The current model took on average 418 s to solve, more

efficient compared to the previous 1D model [9], which took 1014 s to solve using the same setup.

The entrained slow waves demonstrated the same frequency at every point along the 1D model, with the lower frequencies being phase-locked to the pacemaker in the proximal end of the model, i.e., the highest frequency entrained the lower frequencies (Fig. 4(a)). The amplitude of the simulated slow wave with lower intrinsic frequency was approximately 3.7 mV higher than that of the higher intrinsic frequency (Fig. 4).

When the 1D model was decoupled, by reducing the conductivities, entrainment was lost. The loss of entrainment is evident in the loss of phase-locking between the simulated slow waves, with each cell generating slow waves at their respective intrinsic frequencies (Fig. 4(b)). In experimental studies, loss of entrainment and the subsequent dysrhythmia in slow wave activity may contribute to uncoordinated gastric contractions, leading to diminished digestive functions [6].

IV. CONCLUSIONS

A computationally efficient biophysical slow wave cell model was developed and applied to simulate entrainment of gastric slow waves in a 1D model. The simulated result suggested that propagation of slow waves is mediated by a phase-locked system of unique intrinsic frequencies and the integrity of the system depends on tissue material properties such as conductivity. In future, the cell model will be applied to quantitatively predict the mechanisms that underpin slow wave dysrhythmias [9].

REFERENCES

[1] G. Farrugia, Interstitial cells of Cajal in health and disease, Neurogastroenterol. Motil. vol. 20, pp. 54-63, 2008.

[2] T. Ordog, M. Baldo, R. Danko, K. M. Sanders, Plasticity of electrical pacemaking by interstitial cells of Cajal and gastric dysrhythmias in W/W mutant mice, Gastroenterology. vol. 123, no. 6, pp. 2028-40.

[3] D. F. van Helden, D. R. Laver, J. Holdsworth, M. S. Imtiaz, Generation and propagation of gastric slow waves, Clin. Exp. Pharmacol. Physiol. vol. 37, no. 4, pp. 516-24.

[4] G. O'Grady, P. Du, L. K. Cheng, J. U. Egbuji, W. J. Lammers, J. A. Windsor, A. J. Pullan, Origin and propagation of human gastric slow-wave activity defined by high-resolution mapping, Am. J. Physiol. Gastrointest. Liver. Physiol. vol. 299, no. 3, pp. G585-92, 2010.

[5] G. O'Grady, T. R. Angeli, P. Du, C. Lahr, W. J. Lammers, J. A. Windsor, T. L. Abell, G. Farrugia, A. J. Pullan, L. K. Cheng, Abnormal initiation and conduction of slow-wave activity in gastroparesis, defined by high-resolution electrical mapping, Gastroenterology. vol. 143, no. 3, pp. 589-98, 2012.

[6] Z. Lin, I. Sarosiek , J. Forster, I. Damjanov, Q. Hou, R. W. McCallum RW, Association of the status of interstitial cells of Cajal and electrogastrogram parameters, gastric emptying and symptoms in patients with gastroparesis, Neurogastroenterol. Motil. vol, 22, pp. 56-61, 2010.

[7] A. Corrias, M. L. Buist, Quantitative cellular description of gastric sloww wave activity, Am. J. Physiol. Gastrointest. LiverPhysiol. vol. 294, pp. G989-85, 2008.

[8] R. A. Faville, A. J. Pullan, K. M. Sanders, S. D. Koh, C. M. Lloyd, N. P. Smith, Biophysical based mathematical modeling of interstitial cells of Cajal slow wave activity generated from a discrete unitary potential basis. Biophys. J. vol. 96, pp. 4834-52, 2009.

[9] J. B. Youm, N. Kim, J. Han, E. Kim, J. Han, H. Joo, C. H. Leem, G. Goto, A. Noma, Y. E. Earm, A mathematical model of pacemaker activity recorded from mouse small intestine, Philos. Transact. A Math. Phys. Eng. Sci. vol. 364, pp. 1135-54, 2006.

[10] A. Corrias, M. L. Buist, A quantitative model of gastric smooth muscle cellular activation, Ann. Biomed. Eng. vol. 35, no. 9, pp. 1595-607, 2007.

[11] M. S. Imtiaz, D. W. Smith, D. F. van Helden, A theoretical model of slow wave regulation using voltage-dependent synthesis of inositol 1,4,5-trisphosphate, Biophys. J. vol. 83, pp. 1877-90, 2002.

[12] P. Du, G. O'Grady, J. B. Davidson, L. K. Cheng, A. J. Pullan, Multi-scale modeling of gastrointestinal electrophysiology and experimental validation, Crit. Rev. Biomed. Eng. vol. 38, no. 3, pp. 225-54, 2010.

[13] P. Du, G. O'Grady, S. J. Gibbons, R. Yassi, R. Lees-Green, G. Farrugia, L. K. Cheng, A. J. Pullan, Tissue-specific mathematical models of slow wave entrainment in wild-type and 5-HT(2B) knockout mice with altered interstitial cells of Cajal networks, Biophys. J. vol. 98, no. 9, pp. 1772-81, 2010.

[14] J. Gao, P. Du, R. Archer, G. O'Grady, S. J. Gibbons, Farrugia, L. K. Cheng, A. J. Pullan,A stochastic multi-scale model of electrical function in normal and depleted ICC networks, IEEE Trans. Biomed. Eng. vol. 58, no. 12, pp. 3451-5, 2011.

APPENDIX

TABLE II

CELL MODEL PARAMETERS

Parameter	Description	Value
C_m	Membrane capacitance	25 pF
G_{Na}	Maximum Na^+ conductance	8 mS
E_{Na}	Na+ reverse poential	80 mV
$\tau_{f_{Na}}$	Na^+ gating time constant	110 ms
$\tau_{d_{Na}}$	Na^+ gating time constant	10 ms
G_{BK}	K^+ maximum conductance	1.2 mS
E_K	K^+ reverse poential	-72 mV
G_{MCa}	Ca^{2+} maximum conductance	4 mS
E_{Ca}	Ca^{2+} reverse poential	-20 mV
q	Hill coefficient	4
k_{Ca}	Half saturation constant for I_{Ca}	1.4 mM
V_0	Ca^{2+} influx into cytosol	0.22 $\mu M\, ms^{-1}$
V_1	Ca^{2+} influx into cytosol due to IP_3	0.2266 ms^{-1}
V_{M2}	Maximum Ca^{2+} pump into store	3.34 $\mu M\, ms^{-1}$
n	Hill coefficient	2
k_2	Cytosolic Ca^{2+} threshold for V_2	1 mM
V_{M3}	Maximum Ca^{2+} pump from store	44 $\mu M\, ms^{-1}$
w	Hill coefficient	4
k_a	Cytosolic Ca^{2+} threshold for V_3	1 mM
m	Hill coefficient	4
k_r	Cytosolic Ca^{2+} threshold for V_3	2 mM
o	Hill coefficient	4
k_p	IP_3 threshold for V_3	0.65 mM
V_{M4}	Maximum IP_3 nonlinear degradation	0.16 $\mu M\, ms^{-1}$
β	IP_3 synthesis constant	0.000062 ms^{-1}
η	Linear IP_3 synthesis	0.00015 ms^{-1}
u	Hill coefficient	0.05 $mM\, ms^{-1}$
k_4	Half saturation constant	0.5 mM
P_{MV}	Maximum IP_3 synthesis	0.32 $mM\, ms^{-1}$
r	Hill coefficient	8
k_v	Half saturation constant	-60 mV
k_f	Rate constant	0.00006 ms^{-1}
K	Rate constant	0.00066 ms^{-1}

TABLE III

CELL MODEL INITIAL CONDITIONS

Variable	Description	Initial Value
V_m	Membrane voltage	-70.0328 mV
d_{Na}	Sodium conductance gate	0
f_{Na}	Sodium conductance gate	0.9998
Ca_c	$[Ca^{2+}]_i$ cytosol	0.38498 mM
Ca_s	$[Ca^{2+}]_i$ intracellular store	2.46238 mM
IP_3	Inositol trisphosphate	0.4778 mM